Materials Horizons

Accepted Manuscript

ROYAL SOCIETY OF CHEMISTRY

rsc.li/materials-horizons

Rare-Earth Quantum Cutting in Metal Halide Perovskites – a Review

Silvia M. Ferro, Merlinde Wobben, Bruno Ehrler*

Center for Nanophotonics, NWO-Institute AMOLF

Science Park 104, 1098 XG Amsterdam, the Netherlands

Abstract

Ytterbium-doped lead halide perovskite (Yb^{3+}:$CsPbX_3$ with *x* =Cl or Cl/Br) nanocrystals and thin films have shown surprisingly efficient downconversion by quantum cutting with PLQYs up to 193%. After excitation of the perovskite host with high-energy photons, the excited states of two Yb ions are rapidly populated, subsequently emitting lower-energy photons. Several synthesis routes lead to highly efficient materials, and we review the progress on both the synthesis, material quality and applicability of these downconversion layers. For solar cells they could be used to increase the power converted from high-energy photons, and first applications have already shown an increase in the power conversion efficiency of silicon and CIGS solar cells. Applications such as luminescent solar concentrators an LEDs are also explored. With further research to overcome challenges regarding power saturation and stability, this material has great potential for a simple route to enhance solar cells.

*Corresponding author: ehrler@amolf.nl

View Article Online
DOI: 10.1039/D0MH01470B

Introduction

Recently the interest in rare-earth (RE)-based downconversion has been revived by surprisingly high photoluminescence quantum yields (PLQY) in Yb-doped metal halide perovskite materials. The most common compositions constitute Yb-doped cesium lead halide perovskites (Yb^{3+}:$CsPbX_3$ with x =Cl or Cl/Br), where the halide ratio is tuned to make sure the bandgap energy is at least twice as large as the emission energy from the Yb ions. These materials can be synthesized as nanocrystals or thin films. The downconversion in these materials proceeds via sharing the excitation energy in the high-bandgap perovskite between two lower-energy excitations of the Yb ions, thereby converting one high-energy photon into two lower-energy excitations, a process termed quantum cutting (QC). Here we review the progress made in recent years in synthesizing and understanding this material. In Section 1 we introduce QC in halide perovskites, in Section 2 we show the various synthesis methods explored so far. We discuss challenges regarding power saturation in Section 3 and the potential applications of Yb-doped perovskites in Section 4. We finalize the review with suggestions for future research in Section 5.

Section 1: Quantum Cutting in Halide Perovskites

In conventional photovoltaic (PV) devices, absorbed photons can ideally give rise to one electron-hole pair that has the energy of the bandgap of the PV material, regardless of the energy of the incoming photon. Photons with an energy below the bandgap are not absorbed. For higher-energy photons, the excess energy above the bandgap is converted into heat, a loss known as *quantum defect* or *thermalization loss*. These two processes are the main losses leading to the limit of the efficiency of single-junction PVs, the Shockley-Queisser limit. For silicon, with a bandgap of 1.1 eV, this limit is ~30% when Auger recombination is taken into account.[1,2]

Several ways to reduce thermalization losses in solar cells are being explored, including multi-junction (e.g. perovskite/Si tandem) devices and carrier multiplication processes - e.g. multiple exciton generation (MEG) in quantum dots and singlet fission in organic semiconductors.

Multi-junction PV represents the most advanced strategy in terms of power conversion efficiency (PCE), reaching efficiencies above 45%.[3] In a multi-junction solar cell, a high-bandgap PV is placed on top of a low-bandgap PV such as silicon. High-energy photons are absorbed by the top cell and lower-energy photons are transmitted through the top cell and absorbed by the bottom cell. In practice these cells require intricate processing and careful choice of materials. If the two cells are connected in series, the total current density of the device is equal to that of the cell with the lowest current density, so for optimal efficiency the two cells should produce equal photocurrent. The need for recombination layers between the cells also complicates the fabrication. For four-terminal configurations, the current does not have to be matched, but additional conductive layers and contacting leads to more parasitic absorption and makes the fabrication even more involved and costly.[4]

MEG quantum dot solar cells could be fabricated by roll-to-roll processing methods. The MEG yield in (quantum confined) semiconductors is not high enough yet to compete with other PV technologies.[5, 6] In contrast to multi-junction PV, singlet fission could be a purely additive process where the downconverter layer can simply be added on top of a suitable low-bandgap solar cell without changes to the cell itself. As

View Article Online
DOI: 10.1039/D0MH01470B

no current matching is required, singlet fission-based PV allows for less complex device architectures and lower production costs. In that sense it is closest to the application area of QC downconversion layers. Nevertheless, currently the low performance of singlet fission-sensitized devices pose a limit for widespread use.[7,8]

A QC downconverter is typically a purely optical system. It absorbs a high-energy photon and emits multiple photons with lower energy. These lower-energy photons are absorbed by the PV layer below, together with the photons transmitted by the downconverter. A simplified illustration of how QC can improve the spectral coverage of PV cells is shown in Figure 1.

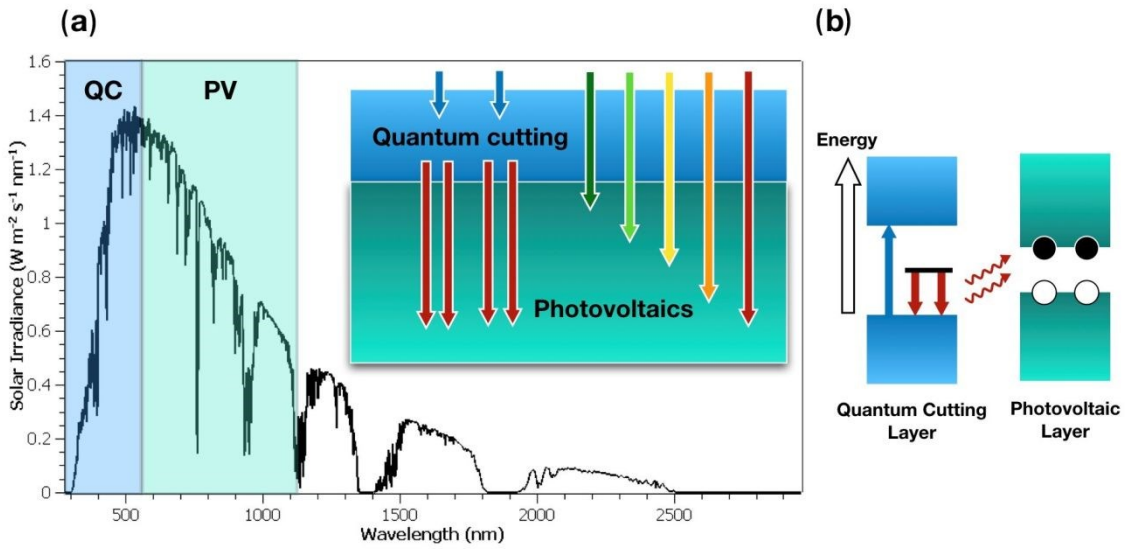

Figure 1. ***(a)*** *Ideal regions for QC and PV absorption in the solar spectrum for a QC PV device and schematic of a QC PV architecture (inset).* ***(b)*** *General mechanism of a QC PV: high-energy light (blue arrow) is absorbed by the QC layer, then converted into two lower-energy photons (red curly arrows) which are then absorbed by an underlying PV, overall generating two excited states per high-energy photon.*

Since QC generates multiple photons per absorbed higher-energy photon, the photoluminescence quantum yield (PLQY) of a QC layer should be higher than unity. Yb-doped perovskites show PLQYs as high as 193%.[9] The atomic states are crucial for understanding the QC process in Yb-based materials. Yb is a rare-earth element of the lanthanide series with atomic number 70. Its most common oxidation state is 3+ with valence electron configuration $4f^{13}5s^25p^6$. The emission from free Yb^{3+} ion comes only from the transition between the two energy levels $^2F_{5/2}$ and $^2F_{7/2}$, with an energy difference of 1.26 eV or 980 nm.[10] According to the Laporte rule, transitions between like atomic orbitals (s–s, p–p, d–d, f–f) are forbidden in a centrosymmetric environment, meaning atoms or molecules with an inversion center. The $^2F_{7/2} - {}^2F_{5/2}$ transition is a Laporte forbidden f–f transition and thus very weak. However, an excitonic transition from a host, for example a perovskite crystal, to Yb^{3+} may lead to population of the $^2F_{5/2}$ state, and this transition is allowed. The excited Yb^{3+} is then long-lived, but eventually emits a low-energy photon with high efficiency.

View Article Online
DOI: 10.1039/D0MH01470B

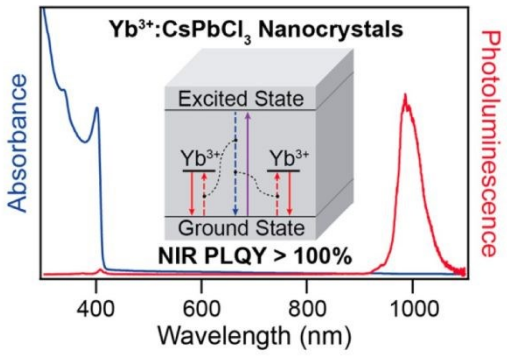

Figure 2. Absorbance and PL spectra of Yb^{3+}:$CsPbCl_3$ nanocrystals. Most of the perovskite emission is quenched when doped with Yb, which then emits twice the flux at around half the energy. Figure used with permission from Milstein et al. [11]

The absorption- and emission spectra of Yb^{3+}:$CsPbCl_3$ are shown in Figure 2. The absorption by the perovskite is in the higher-energy part of the spectrum, starting above twice the emission energy. The emission at around 1.26 eV is close to the bandgap of silicon at 1.1 eV where the EQE is still high (at least for silicon cells with good light management) and the thermalization losses are small.

For most examples of RE QC the absorption onset starts around 400 - 450 nm while the ideal onset for a silicon-based downconversion solar device is 550 nm, twice the silicon bandgap. This mismatch reduces the efficiency potential. However, perovskite compositional tuning allows to push the absorption onset to lower energies for QC,[12] and a QC material with an absorption onset of twice the bandgap of silicon has an efficiency potential similar to two-terminal tandem solar cells.[8,13]

Mechanisms

QC proceeds by populating two Yb $^2F_{5/2}$ states in the perovskite host following perovskite excitation. Two different mechanisms were initially proposed for the population of the $^2F_{5/2}$ state in Yb^{3+}:$CsPbCl_3$. Milstein *et al.* proposed a mechanism where a shallow lattice defect induced by the dopant Yb leads to a rapid depopulation of the host. Electrons can relax into the defect state and then recombine with the valence band while transferring energy to two Yb ions, generating two excited $^2F_{5/2}$ – $^2F_{7/2}$ transitions.[11] To test this hypothesis, both Yb^{3+}:$CsPbCl_3$ NCs and La^{3+}:$CsPbCl_3$ NCs were fabricated. La^{3+} is very similar to Yb^{3+} but shows no optical emission. At 4.7 K, La^{3+}:$CsPbCl_3$ shows emission 40 meV below the excitonic PL of undoped $CsPbCl_3$ NCs. This emission is not observed for undoped NCs, suggesting the introduction of a shallow defect state upon doping with a lanthanide.

Pan *et al.* proposed a mechanism that involves a deeper defect, closer to the middle of the bandgap. After photoexcitation, excitations in the host can share their energy between the defect and one Yb^{3+} ion and populate one $^2F_{5/2}$ excited state. Then the electron in the defect state can recombine with the valence band of the host lattice and transfer its energy to the second Yb^{3+} ion to populate another $^2F_{5/2}$ excited state.[14] Emission spectra for Yb^{3+}:$CsPbCl_3$ were collected at 300 K and 10 K to test this hypothesis. At 10 K there is an additional broad component centered at 596 nm that is not there at room-temperature. According to Pan *et al.* this is consistent with emission from a defect state between the conduction and the valence band. We

View Article Online
DOI: 10.1039/D0MH01470B

note that this emission is at an energy much larger than half the bandgap, and unless the energetics change dramatically at room temperature, this model would not fulfill the requirement of energy conservation.

To further disseminate the two mechanisms, density functional theory (DFT) calculations were carried out on the cubic phase of Yb^{3+}:$CsPbCl_3$ NCs to investigate the properties of the system. These calculations supported the mechanism involving a shallow defect state.[15]

Dopant-induced Defects and Charge Balance

The depopulation of the excited states in the perovskite host occurs on the picosecond timescale, suggesting that the dopant introduces defects in the host lattice itself.[11] To be incorporated in the lattice, the Yb^{3+} ion must take the position of another ion. Pan *et al*. carried out DFT calculations to study the position of the Yb^{3+} ions in the perovskite structure by calculating the formation energy of three different defects in the perovskite. From the three defects, at the interstice, at the location of Cs, and at the location of Pb, the formation energy of the Pb defect was always the lowest. This is a first indication that Yb^{3+} ions will tend to occupy the Pb^{2+} site.[14]

Since the valency of Yb and Pb is different (3+ and 2+ respectively), charge compensation is necessary upon incorporation of Yb^{3+} into the lattice. Charge compensation can be realized by the introduction of two different cation vacancies, V_{Cs} or V_{Pb}, into the lattice. Upon higher nominal Cs concentrations during synthesis, which should reduce V_{Cs} formation, the PLQY from Yb increases. This implies that lead vacancies are formed for charge balance. Thus, Milstein *et al.* suggest a charge-neutral Yb^{3+}–V_{Pb}–Yb^{3+} defect complex that takes the place of three Pb ions, where QC is aided because there is always a shallow V_{Pb} defect near a pair of Yb^{3+} ions.[11] The proximity of the vacancy to the Yb^{3+} ions in this configuration provides electronic coupling of the defect to both Yb^{3+} ions because the Bohr radius of the V_{Pb}-localized photogenerated charge carriers is so large that is spans the vacancy-defect complex.

More evidence for a vacancy-defect structure was provided by Erickson *et al.*. They considered two different scenarios; one where QC involves a Yb^{3+}–V_{Pb}–Yb^{3+} complex and one where it involves any two Yb^{3+} ions in a nanocrystal. In the first scenario, the effective QC rate, and therefore the PLQY, is linearly correlated with the number of ground state Yb^{3+} ions while in the second scenario the QC is not linearly correlated with the Yb^{3+} concentration because there are many more possible pairwise combinations of Yb^{3+} ions at higher concentrations. Experimentally, the PLQY is linearly correlated with Yb concentration, favoring the hypothesis of a vacancy-defect structure.[16]

View Article Online
DOI: 10.1039/D0MH01470B

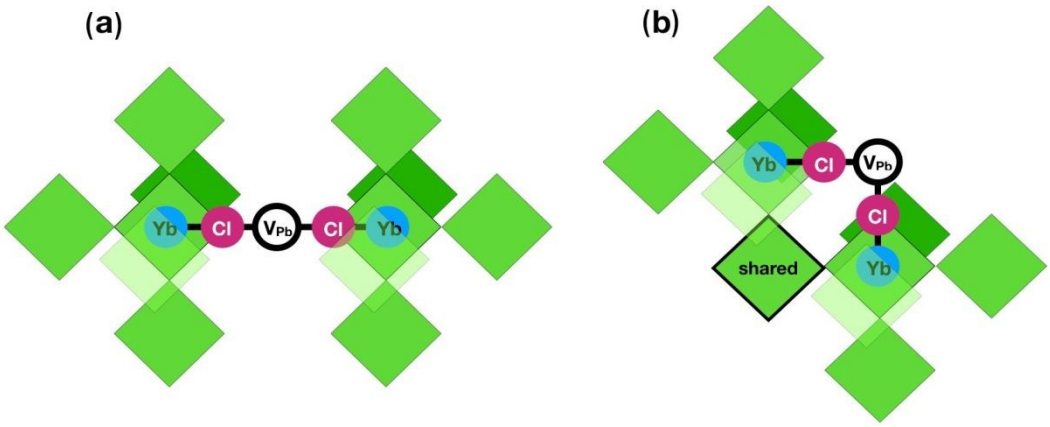

Figure 3. Possible defect-complex configurations. ***(a)*** *A linear configuration involves 10 distorted octahedra upon doping with Yb.* ***(b)*** *In a right-angle configuration, the number of distorted octahedra is 9, because one ochtaedron is shared between two doped structures.*

The charge balance is achieved by replacing three Pb^{2+} ions with one pair of Yb^{3+}. This pairwise configuration could be achieved by various structural arrangements. Li *et al.* compared the energies of five random configurations of a Pb vacancy with two Yb^{3+} ions to a linear configuration using DFT and found that the linear configuration had lower energies than the random configurations. They further compared the energies of a linear and right-angle (RA) configuration, which showed that the RA configuration is more stable than the linear configuration.[15] An intuitive picture, illustrated in Figure 3, explains this difference. Pure $CsPbCl_3$ perovskite consists of $PbCl_6$ octahedra surrounding the Cs cations. In a linear Yb^{3+}–V_{Pb}–Yb^{3+} defect complex, both Yb^{3+} ions are bound to five $PbCl_6$ octahedra that will be distorted. The linear configuration thus distorts ten octahedra. In contrast, in a RA configuration one of the $PbCl_6$ octahedra is distorted by both Yb^{3+} ions, so the total number of distorted octahedra is nine. Therefore, the RA configuration is more stable than a linear configuration. However, the energy difference is relatively small (100 meV), so both configurations may coexist at room temperature.

Section 2: Synthesis Methods

QC in Yb-doped perovskites has been demonstrated for nanocrystals (NCs) and thin films. The published synthesis methods are summarized in Table 1. Most methods for Yb^{3+}:$CsPbX_3$ perovskite NC synthesis are based on a hot injection method. Typically a Cs-oleate precursor is swiftly injected into Pb and Yb precursors at elevated temperatures. The reaction is quenched after the desired growth time, for example in an ice bath, and the halide mixture can be controlled by (partially) using Pb halides as a Pb precursor. With this procedure, the doping ions are integrated in the perovskite lattice during the synthesis of the NCs.[11,14,16–22] It is also possible to incorporate Yb post-synthetically by ion exchange reactions.[23]

Table 1. Summary of synthesis methods and the resulting PLQYs.

Doped perovskite composition	Synthesis highlights		PLQY (%) [Fluence]	Ref.
	Method	Precursors*		
Thin-film				
Yb^{3+}:$CsPb(Cl_{0.35}Br_{0.65})_3$	2-step spin coating	YbX_3, PbX_2, CsX	193 [~3 x 10^{13} cm^{-2} s^{-1}]	9
Yb^{3+}:$CsPb(Cl_{0.5}Br_{0.5})_3$	SSVD	YbX_3, PbX_2, CsX	183 [NA]	24
Nanocrystals				
Yb^{3+}:$CsPbCl_3$	Hot injection	1. $(YbOAc)_3$, $Pb(OAc)_2$, CsOAc 2. TMS-Cl	170 [~30 NC^{-1} s^{-1}]	11
Yb^{3+}:$CsPbCl_3$	Hot injection	1. $YbCl_3$ 2. $PbCl_2$ 3. CsOA	143 [NA]	14
(Yb^{3+}, Pr^{3+}, Ce^{3+}):$CsPbClBr_2$	Hot-injection	1. $YbCl_3$, $PrCl_3$, $CeCl_3$ 2. $PbCl_2$ 3. CsOA	173 [NA]	20
Yb^{3+}:$Cs_2AgInCl_6$	Hot injection	1. $(YbOAc)_3$, $CsCO_3$, AgOAc, $In(OAc)_3$ 2. TMS-Cl	3.4 [NA]	25
Yb^{3+}:$Cs_2AgInCl_6$ Er^{3+}:$Cs_2AgInCl_6$	Hot injection	1. $(LnOAc)_3$, $CsCO_3$, AgOAc, $In(OAc)_3$ 2. TMS-Cl	3.6 [NA] 0.05 [NA]	26

*For NCs, precursors listed in order of addition to reaction flask for dissolution/reaction at high temperature.

The nature of the precursors employed in the NC synthesis may play a role in the final QC efficiency. For example, Milstein et *al.*[14] used metal acetates instead of metal halides, because of their higher solubility in the long-chain organic solvents employed in the NC synthesis and the PLQY is slightly lower than the other NC syntheses. However, no systematic study has been conducted on the exact relation between the choice of the precursors and PLQY yet.

A one-pot method was developed using ultrasonication, however, the reaction yield is lower and the NC size distribution broader compared to the hot-injection method. [27]

When grown as thin films, Yb-doped $CsPbX_3$ perovskite is fabricated by a 2-step spin coating procedure. First, a $PbCl_2$ precursor is spin-coated and annealed. Then, a Cs and YbX_3 precursor is spun onto the heated substrate and subsequently annealed at 250 °C.[9]

A solvent-free route to prepare thin films using a Single-Source Vapor Deposition (SSVD) method was also investigated. The precursors are ground mechanochemically for nine hours to yield powder perovskites, which are then used as source materials for SSVD.[24]

Because of Pb toxicity concerns, methods have been developed to synthesize Yb-doped perovskites without Pb. These synthesis paths all use a hot-injection method, and successful examples include $Cs_2AgInCl_6$,[25,26] and $Cs_2AgBiCl_6$.[28]

View Article Online
DOI: 10.1039/D0MH01470B

Perovskite Composition and Yb Doping Level

For efficient QC to occur, fine tuning of the properties of the materials is crucial. For example, as the PL energy of Yb is fixed at 1.26 eV, in order for QC to be efficient the host material bandgap must be > 2 × 1.26 eV (> 2.52 eV).[12] One of the advantages of using halide perovskites is their bandgap tunability, predominantly achieved by changing the halide mixing ratio. In fact, by mixing Cl^- and Br^- in the perovskite composition, the bandgap is tuned between 2.32 eV and 2.99 eV - for $CsPbBr_3$ and $CsPbCl_3$, respectively. For $CsPb(Cl_{1-x}Br_x)_3$, a bandgap equal to 2.52 eV corresponds to x = 0.84.[12] Therefore, any $x < 0.84$ would enable QC, with decreasing yields as x increases above the 0.84 threshold. This trend is confirmed by experimental studies where the PLQY is measured as a function of the halide ratio, both for thin film and NC architectures. In particular, for thin films with x = 0.0, 0.41 and 0.65 PLQY values up to 193% were achieved, and dropped below 100% for $x \geq 0.87$.[9] Yb^{3+}:$CsPb(Cl_{1-x}Br_x)_3$ NCs were studied by Milstein et al., showing a steep drop in PLQY at x > 0.75,[29] slightly below the expected cut-off.

Yb doping levels also play a crucial role in determining the efficiency of QC. In general, the PLQY of the $^2F_{5/2} \rightarrow {}^2F_{7/2}$ transition from Yb increases with Yb concentration.[11] For doping levels between 0 and 7.4%, the PLQY rises about linearly with the Yb concentration. Interestingly, higher doping levels have proven to be difficult to achieve. For thin films, a nominal precursor ratio of [Yb]:[Cs] = 1:1 leads to an analytical doping level of 13.3% - and, again, the highest PLQY was measured for the highest Yb concentration.[9] Difficulties in realizing higher dopant concentrations are presumably due to changes in the host lattice structure with increasing doping levels.[11] For example, it was shown that the degree of crystallinity of RE-doped $CsPb(Cl_{0.5}Br_{0.5})_3$ NCs is lowered compared to corresponding undoped NCs, with the perovskite structure partially destroyed at high dopant concentrations.[18]

Mir *et al.* introduced a post-synthetic method where Yb is incorporated in the perovskite lattice after synthesis of the NCs. However this led to low analytical dopant concentrations – i.e. 0.6% and 0.7% for $CsPbCl_3$ and $CsPbBr_3$, respectively.[23] The highest reported nominal-to-analytical dopant concentration was achieved by Crane et *al*. via SSVD, leading to 4.7% Yb when the nominal concentration was 5.0%.[24]

Lanthanide Co-doping and Pb-free Double Perovskite

Most of current research on QC focuses on doping perovskites with Yb. Nonetheless, early works on Yb doping of perovskites showed that co-doping with a second lanthanide might be beneficial to achieve higher QC efficiencies.

For example, Zhou et *al.* originally showed that adding 2% Ce to 7.1%-Yb-doped $CsPbCl_{1.5}Br_{1.5}$ rises the PLQY from 115% to 146%.[18] In a follow-up work, perovskite NCs were doped with Ce and Pr in addition to Yb, leading to a PLQY as high as 173%.[20] For this tridoped system a mechanism of the improvement of QC efficiency was proposed, schematically illustrated in Figure 4. Ce^{3+} ions serve as an intermediate energy level promoting energy transfer from the perovskite host to Pr^{3+}. Electrons on the $^3P_2$ level of Pr^{3+} transit non-radiatively to $^3P_0$ and $^1D_2$ of Pr^{3+}. These can then emit through $^3P_0 - {}^3F_2/{}^3H_4$ and $^1D_2 - {}^3H_4$ transitions. As evidenced by emission spectroscopy at various (co-)doping levels, QC via Yb^{3+} is achieved by a cross-

relaxation [Pr^{3+} ($^3P_0$ – $^1G_4$);Yb^{3+} ($^2F_{7/2}$ – $^2F_{5/2}$)] and a second energy-transfer process [Pr^{3+} ($^1G_4$ – $^3H_4$);Yb^{3+} ($^2F_{7/2}$ – $^2F_{5/2}$)]. A second QC process occurs as the energy is transferred from one Ce^{3+} ion to two Yb^{3+} ions - a transfer enabled by the fact that the $5d$ – $^2F_{5/2}$ of Ce^{3+} is exactly twice the energy of the $^2F_{7/2}$ – $^2F_{5/2}$ transition of Yb^{3+}.

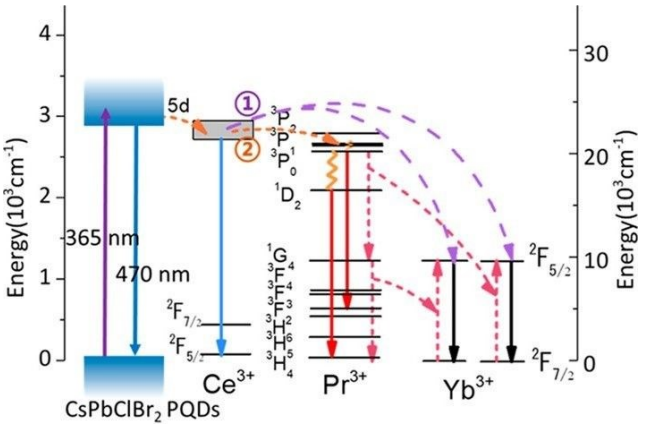

Figure 4. Kinetic scheme for the mechanism of excitation and quantum-cutting in Yb^{3+}, Pr^{3+}, Ce^{3+}:$CsPbClBr_2$ tridoped NCs. Figure used with permission from Zhou et al.[20]

Due to increasing concerns about Pb toxicity, substantial research efforts aim at developing perovskite-based solar cells with low or no Pb content. Double perovskites (DP), with the structure $A_2M^+M^{3+}X_6$ use two different metals alternating with valency 1+ and 3+ to replace the Pb^{2+} (Figure 5). Previous reports have shown a higher stability of this structure compared to Pb halide perovskites,[30] however, this may vary depending on a number of factors, including halide composition.[31]

Double perovskite NCs were also doped with lanthanide ions. Lee *et al.* studied $Cs_2AgInCl_6$ NCs doped with Yb and Er. Although the synthesis was successful, the doping level achieved was particularly low, with a nominal Yb concentration of 20% corresponding to an analytic doping level of 0.9% and a PLQY of 3.4%.[26] Yb-doped $Cs_2AgInCl_6$ NCs and microcrystals were synthesized by Mahor *et al.,* and while a higher Yb uptake was achieved (nominal 52% Yb led to an analytical value of 6.2%) the corresponding PLQY does not exceed that of Pb-based perovskite - absolute numbers are not reported but the PLQYs of both NCs and microcrystals are more than an order of magnitude smaller than that of Yb -doped $CsPbCl_3$ NCs synthesized by the same group.[25] Chen *et al.* compared Yb-doped $Cs_2AgBiCl_6$ and $Cs_2AgBiBr_6$ NCs. A nominal Yb concentration of 7.7% led to an analytical concentration of 5.5% and 5.0% in $Cs_2AgBiCl_6$ and $Cs_2AgBiBr_6$, respectively.[28] As the PLQYs of these NCs are not reported, QC efficiencies in $Cs_2AgInCl_6$ and Cs_2AgBiX_6 cannot be directly compared.

In general, the reason for the lower PLQY in RE-doped DPs may lie in the absence of the formation of the vacancy-defect complex that forms in lead halide perovskites where the 2+ valency of Pb requires the replacement of three Pb ions with two Yb^{3+} ions. Both In and Bi have a valency of 3+ and we thus suspect that Yb^{3+} ions most easily take the place of In or Bi, without the formation of two Yb^{3+} ions in close proximity. If no vacancy-defect complex is formed, there is also no vacancy to assist the population of the Yb^{3+} excited state. Therefore, QC may be absent or inefficient in DPs.

View Article Online
DOI: 10.1039/D0MH01470B

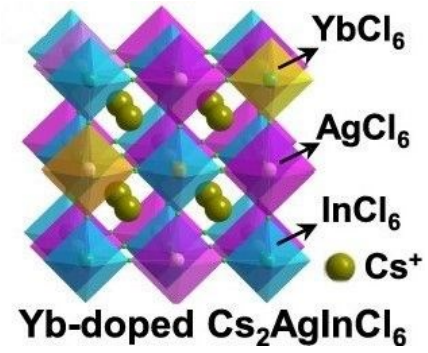

Figure 5. Structure of a Yb-doped $CsAgInCl_6$ double perovskite. Figure used with permission from Mahor et al..[25]

Nanocrystals or Thin Films?

A substantial portion of Yb-doped perovskite research focuses on NCs. However, the highest reported PLQY of 193% was achieved in a thin film architecture.[9] While this study shows that QC is a bulk effect, we know little about the advantages or disadvantages of the two different architectures because only two reports of thin films are currently available, without a direct comparison to NCs.

On a practical level, thin films are easier to synthesize, involving a 2-step spin coating procedure, while NCs are most often prepared by hot injection method (Table 1) and then spin-coated or drop-casted to form a film. As-synthesized Yb-doped $CsPbX_3$ NC solutions also need to undergo multiple washing and dilution cycles to remove impurities, unreacted species and excess of long-chain organic components. Interestingly, although this is a disadvantage from a practical point of view, the QC performance is not affected by the washing procedure. One washing step already reduces the excitonic perovskite NC emission by 70%, but the NIR PL stays around 90% of its initial value after up to four washing cycles.[11]

Thin films of mixed lead halide perovskites undergo phase segregation creating Br-rich and Cl-rich phases.[32] The resulting change in bandgap may be problematic for QC because the bandgap of the Br-rich phase is lower than twice the energy of the $^2F_{7/2} - {}^2F_{5/2}$ transition of Yb^{3+}. Fortunately, QC may help reduce phase segregation. Kroupa et *al.* observed phase segregation in their $CsPb(Cl_{1-x}Br_x)_3$ thin films, but for the Yb-doped $CsPb(Cl_{1-x}Br_x)_3$ thin film this segregation was strongly suppressed due to rapid energy capture by Yb^{3+}, avoiding the driving force for halide segregation.[9]

Section 3: Power Saturation

One of the most extensively reported limiting factors for Yb-doped perovskites to achieve widespread use is their power saturation effect at relatively low excitation intensities, both in NCs and thin films. The PLQY drops well below 100% at higher intensities, diminishing the potential photocurrent gain from QC.

Figure 6 shows the PLQY of Yb^{3+}:$CsPb(Cl_{1-x}Br_x)_3$ at varying excitation intensities, both for thin films and nanocrystals. As shown in *Figure 6*a, power saturation significantly reduces the PLQY of Yb-doped lead halide perovskite thin films[9] well below the excitation flux of AM1.5 solar irradiation in the range between 280-490 nm (3.4×10^{16} cm^{-2} s^{-1}). Interestingly, this effect is almost independent of the perovskite (NC)

View Article Online
DOI: 10.1039/D0MH01470B

halide composition: even for compositions with *x* close to 1, which have low PLQYs because the bandgap is too low for QC to be efficient, Erickson et al. observed a nearly identical power saturation trend – Figure 6b, full (x = 0) and empty (x = 0.9) blue circles.[16] Milstein et al. reported a similar PLQY decrease for Yb-doped $CsPbCl_3$ NCs in the fluence range between ~ 30 and 500 s^{-1} [11] (*Figure 6*b, green triangles). The difference in the fluence-dependence of the PLQY reported for Yb^{3+}:$CsPbCl_3$ NCs by Milstein et al.[11] and Erickson et al.[16] is possibly due to the different scale along the y-axis and/or to the different way the PLQY values were obtained.

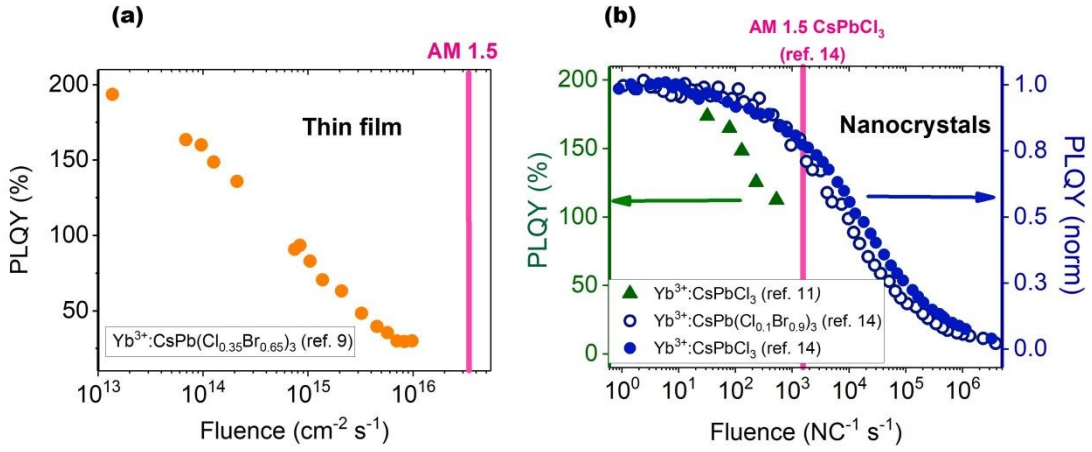

Figure 6. NIR PLQY of Yb^{3+}:$CsPb(Cl_{1-x}Br_x)_3$ as function of the fluence. (a) Measured PLQY for thin films with x = 0.65. (b) PLQY, normalized to the average emission value in the low photoexcitation power limit, for NCs with x = 0 (blue full circles) and x = 0.9 (blue empty circles); measured PLQY (%) for Yb^{3+}:$CsPbCl_3$ NCs (green triangles). Data from Kroupa et al.,[9] Erickson et al.,[16] and Milstein et al.,[11] respectively.

A number of mechanisms were proposed for the power saturation, based on the notion that this effect must involve a non-radiative relaxation occurring when a NC containing an excited Yb^{3+} ion is excited again. Milstein *et al.* attributed the saturation to a combination of the large absorption cross-section of $CsPb(Cl_{1-x}Br_x)_3$ and the very long average Yb^{3+} PL decay time of $\tau > 2$ *ms*.[11]

The kinetic model developed by Erickson et al. ascribes the effect to the two Auger-type processes with which the relaxation to the ground state via luminescence will have to compete.[16] A schematic illustration of this mechanism is shown in Figure 7. In the first process, A1, the energy from the excited Yb^{3+} ion is transferred to the NC which creates a hot exciton and a ground-state Yb^{3+} ion. The hot exciton will thermally cool to the band edge. In this process, the energy of one $^2F_{5/2} - {}^2F_{7/2}$ transition of Yb^{3+} is lost. In the second competing process, A2, the energy of the NC is transferred to the excited Yb^{3+} ion, which generates a highly excited Yb^{3+} ion and a NC ground-state. The highly excited Yb^{3+} ion can relax thermally to the $^2F_{5/2}$ state, and emit a photon from that state. In this process, the energy of roughly one $^2F_{5/2} - {}^2F_{7/2}$ transition is lost.

The power dependence of the PLQY, simulated with a kinetic model based on these competing processes, shows that A2 closely matches the experimental saturation curves by kinetically out-competing QC, with no significant contribution from A1. Finally, the simulations show that QC out-competes the cross-relaxation process until 20% of Yb^{3+} ions are in the $^2F_{5/2}$ state.

View Article Online
DOI: 10.1039/D0MH01470B

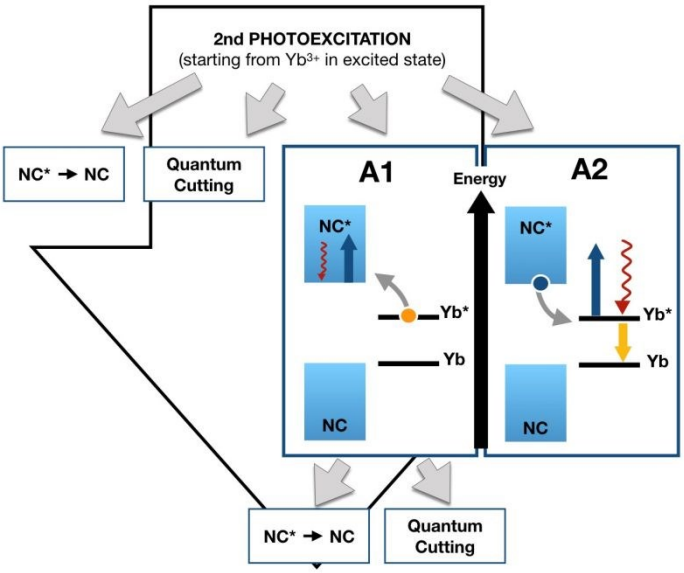

Figure 7. Kinetic schemes for two processes of non-radiative relaxation (A1 and A2) of an excited Yb^{3+} ion, leading to power saturation. Based on Erickson et al.[16]

Section 4: Applications

Downconversion Layer

The most widely reported application of RE-doped perovskite is as a downconversion layer. The working principle of this application, schematically illustrated in Figure 8a, consists in the absorption of the high-energy light by the downconversion material before it reaches the underlying solar cell. The layer then converts each photon into multiple photons of lower-energy light in a spectral regime where the solar cell performs more efficiently. Thus, the downconversion layer has two advantages for these cells, the photon multiplication by QC, and the down-conversion of the high-energy photons to an energy range where the EQE of the solar cell is higher. Devices with such design hence show strong improvement in photoelectric response between 350 and 450 nm, corresponding to the absorption range of the perovskite used.[18,20]

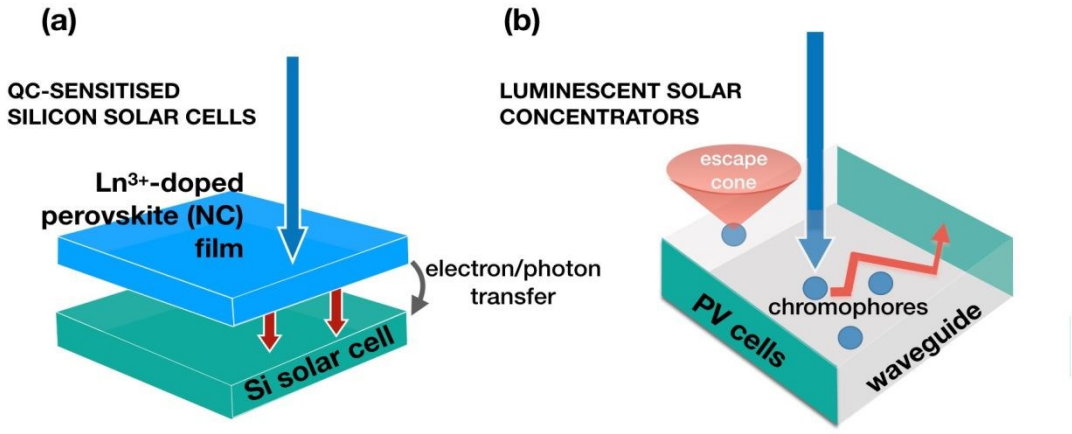

Figure 8. Quantum cutting-based photovoltaic applications. ***(a)*** *Schematics of a QC-sensitized Si solar cell. Improved solar energy conversion efficiency can be achieved efficient QC and effective electron/photon transfer from the downconversion layer to the underlying silicon solar cell.* ***(b)*** *Illustration and working principles of an LSC. Short wavelength radiation is absorbed by downconversion chromophores and re-emitted at longer wavelengths. These are guided to the PV cells at the edges of the waveguide by total internal reflection.*

Zhou *et al.* first reported on the use of Yb-doped perovskite NCs to improve the silicon solar cell efficiency.[18] In their work, the NCs were self-assembled via liquid-phase deposition onto a 125 × 125 mm monocrystalline silicon solar cell. The downconversion film thickness was varied from 60-770 nm. They found that the transmittance of light decreased with increasing thickness. For thickness values below 230 nm the below-bandgap transmittance was as high as 80-90%. The uncoated silicon solar cell had a PCE of 18.1%, which increased to 21.5% when coated with 230 nm of doped perovskite NCs.

In a more recent work by the same group, a commercial $CuIn_{1-x}Ga_xSe_2$ (CIGS) solar cell was coated with (Yb^{3+}, Pr^{3+}, Ce^{3+}):$CsPbClBr_2$ NCs, increasing the PCE of the cell from 15.9 to 19.1%. A 36 x 21 cm solar cell with the same architecture was used to charge a mobile phone, reducing the charging time (0 – 100 % battery charge) by 30 min compared to the corresponding uncoated CIGS solar cell. Similarly, the PCE of a silicon solar cell coated with the same tridoped-$CsPbClBr_2$ NCs increased from 18.1 to 21.9%.[20]

To investigate the extent of the power saturation effect on a QC-sensitized PV device under real-world conditions using Yb^{3+}:$CsPb(Cl_{1-x}Br_x)_3$ as a downconversion material, Crane *et al.* performed detailed balance modeling.[12] In their model, the bandgap energy and PLQY of the downconversion layer were varied, together with the solar cell EQE, the PL capture efficiency following QC (optical coupling, OC), seasonal and daily variations in solar irradiance and saturation effects of the downconversion material. Then, they calculated hourly PLQY, energy yield and efficiency of the devices. Their results show that the solar cells benefit from QC at each daylight hour, despite power saturation effects (*Figure 9*). The highest PLQY improvement is observed in winter - at dawn or dusk - when solar irradiance (hence, power saturation) is lowest. The comparison between two different locations, Seattle, WA (USA) and Golden, CO (USA), is shown in *Figure 9*b. Golden has a much higher fraction of direct illumination and has hence a larger overall energy yield, but the relative gain from the QC layer is only slightly lower than the values in Seattle where the irradiation is weaker. This comparison shows that the differences in power saturation considered in this example do not affect the overall power gain significantly. In absence of any power saturation effect, the device annual energy yield would increase by 20.6%, a significant improvement, which is also comparable to the results by Zhou *et al*..[18] Power saturation with 100% OC decreases the energy yield gain to 12.7%. Also a 2-axis tracking of the Sun is considered and the relative performance increases are similar for tracked and stationary solar cells

More interestingly, even at only 50% OC, the model predicts an annual energy yield improvement of about 2%. In this case, when the potential improvement from QC (i.e. doubling of photons reaching the silicon solar cell) should be cancelled by halving the OC, the benefit of using Yb-doped perovskite NCs as a downconversion layer derives from spectral conversion: high-energy photons are converted into lower-energy photons, which the considered silicon cell absorbs more efficiently. This effect is emphasized by the silicon heterojunction cell simulated here, where the performance in the blue and UV is very poor with an

View Article Online
DOI: 10.1039/D0MH01470B

EQE dropping to below 50% at 3.5 eV incident photon energy. More efficient solar cells, for example Si cells based on n-type cast-monocrystalline wafers often have better blue response, well above 80% in the same energy range.[33] In practice, if the QC layer is in direct contact with the solar cell or module, the difference in refractive index of air and silicon will guide the photons towards silicon, leading to an effective OC well above 50%.

We note that, although the model described suggests that the power saturation effect does not constitute a major limiting factor for the application of Ln-doped perovskites as a downconversion material, some experimental power saturation trends (*Figure 6*) show a large drop in PLQY at light intensities below 1% of the 1 Sun irradiance. This penalty seems to be more severe for thin films, suggesting that in practice power saturation may pose a significantly heavier drawback in these materials.

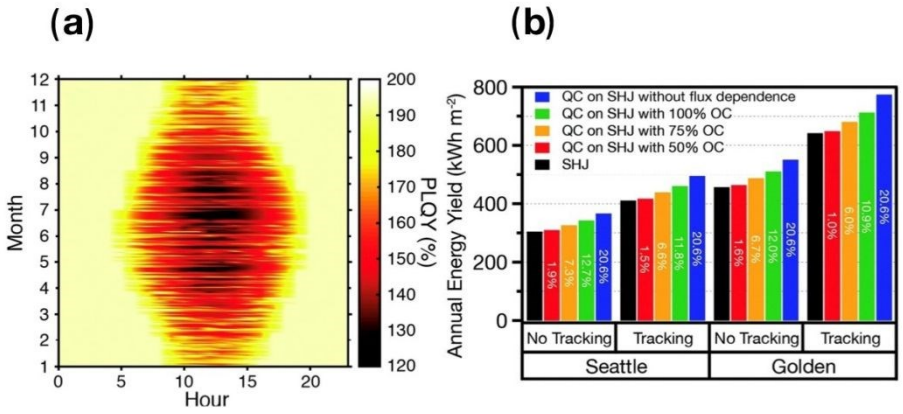

Figure 9. ***(a)*** *Hourly PLQY of the downconversion layer, simulated in Seattle over the course of a year.* ***(b)*** *Energy yield of a* Yb^{3+}*:*$CsPb(Cl_{1-x}Br_x)_3$*/silicon heterojunction (SHJ) device with and without 2-axis tracking for Seattle and Golden, and at different optical coupling (OC) efficiencies. Figure used with permission from Crane et al.*[12]

Luminescent Solar Concentrators and Light-Emitting Diodes

Another possible application of Yb^{3+}:$CsPb(Cl_{1-x}Br_x)_3$ NCs is in the field of Luminescent Solar Concentrators (LSCs). As shown in Figure 8b, in an LSC incident sunlight is absorbed by chromophores embedded in large collector sheets, re-emitted by waveguided photons, transmitted to the edges by total internal reflection. Solar cells placed at the edges can then absorb this light. Advantages of using this technology include reduction of costs (especially compared to III-V PVs) thanks to the reduced PV surface area, and the possibility of integration into (semi)-transparent solar windows. The concentration of sunlight could, in principle, also lead to a higher power conversion efficiency of the solar cell.

As also highlighted by Ferreira et al.[34] and Mir et al.[35], a common problem in LSCs is the reabsorption of emitted photons as they transmit towards the edges of the device, which lowers the quantum efficiency. With QC, the Stokes shift is very large, dramatically reducing the re-absorption problem. This large Stokes

shift is achieved because the emission comes from the Yb^{3+} f-f transition that has very little oscillator strength (also leading to the long emission lifetime). Luo *et al.* reported the fabrication of a 25 cm^2 QC-sensitized LSC using Yb^{3+}:$CsPbCl_3$ NCs with an internal quantum efficiency of 118%, potentially leading to an EQE of 6.3% if integrated into a 1 m^2 window - four times as high as the current record.[22]

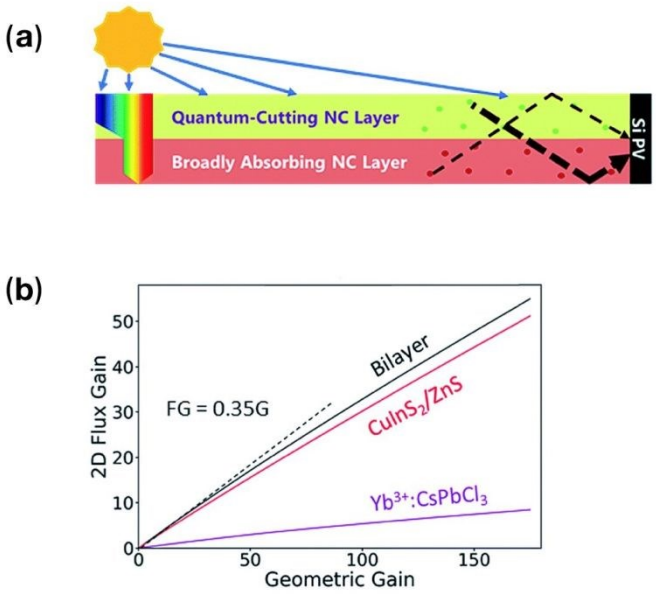

Figure 10. ***(a)*** *Schematics of a bilayer LSC and* ***(b)*** *quantification of improved performance compared to single-layer LSCs. Adapted from Cohen et al.* [17]

One of the limiting factors for QC-sensitized single-layer LSCs lies in the narrow absorption of Yb^{3+}:$CsPb(Cl_{1-x}Br_x)_3$ NCs. In previous works this has been addressed by designing an LSC where an additional absorbing material and waveguide are included, in a tandem architecture. Cohen *et al.* further developed this concept, proposing a model of a bilayer LSC device where, in contrast with tandem LSCs, photons from *both* layers are all directed by the same waveguide to the same PV (Figure 10a), reducing costs and complexity of the architecture.[17] The results of this model (Figure 10b) show the improved performance of the bilayer device compared to its individual components. The flux gains are plotted as a function of the geometric gain for each system and the performance is determined by the slope of the corresponding curves. For a bilayer device where Yb^{3+}:$CsPbCl_3$ is employed, this slope is equal to 0.35 - compared to 0.06 and 0.32 for the monolayer perovskite and $CuInS_2$ LSCs, respectively. The improvement is even higher when using doped mixed halide perovskites with the composition Yb^{3+}:$CsPb(Cl_{0.25}Br_{0.75})_3$. The flux-gain slope of the bilayer device increases from 0.35 to 0.43, with a flux gain equal to 63 at a geometric gain of 175. This means that, for the modelled 70 x 70 x 0.1 cm^3 bilayer LSC, the 28 cm^2 silicon solar cells at the edges of the LSC would generate 63 times more current than during operation without any solar concentration. These results constitute certain advantages for widespread use of this device design for example flexibility in appearance and possibility to be integrated into windows. However, the overall power conversion efficiency per area is lower than the silicon cells alone, and production costs may not be able to compete with the very low costs of solar cells nowadays.

In addition to applications in solar cells and LSCs, RE-doped perovskites could be used in light-emission applications. For example, lanthanide co-doping of $CsPbCl_3$ NCs could serve as an effective way to produce stable white LEDs. Coating a commercial UV-emitting LED emitting at 365 nm with (Ce^{3+},Mn^{2+}):$CsPb(Cl_{0.6}Br_{0.4})_3$ NCs leads to white light at a luminous efficiency of 51 lm/W.[36] As reported by Ishii et al, highly efficient LEDs can also be achieved using Yb^{3+}:$CsPbCl_3$ thin films, exhibiting an EQE of 5.9% with a peak wavelength at 984 nm.[37]

Section 5: Outlook

QC in LHPs has already made astonishing progress within a very short time-span and within a limited number of research groups. Applications, especially for solar cells, seem around the corner. The near future will show if QC can indeed be used to increase solar cell efficiency on the large scale. Practical barriers, such as a conservative industry, stability and toxicity issues, and the actual implementation in solar cells will be much easier to solve once more clarity about the fundamental mechanisms of degradation, the QC process itself, and the power saturation becomes available. The field offers ample space for both fundamental and applied research, and below we outline some of the most pressing challenges.

Efficiency Optimization

As with any application where efficiency matters, more research should be conducted to optimize the performance of the Yb-doped perovskite. One handle is to further optimize the perovskite composition. For example, it was calculated that the optimal mixing ratio x in $CsPb(Cl_{1-x}Br_x)_3$ should be ~0.84,[12] but the values closest so far are 0.75[20] and 0.87[9]. Another handle of efficiency optimization is the doping percentage of Yb. In all examples so far the PLQY of Yb-doped perovskites increases for increasing Yb concentration. This trend presumably has a structural limit because with every two Yb^{3+} ions a defect is introduced into the lattice. Pushing the material towards this limit contains synthetic challenges, and could involve theoretical calculations or variations in the cation mixture to allow higher defect concentrations by incorporating cations of different sizes.

Stability and Pb Toxicity

Materials stable for several decades are required for any large-scale application in solar cells. Photodegradation of LHPs is a well-known issue and the mechanism is not fully understood yet.[38] $CsPbX_3$ NCs show fast decrease in PLQY upon exposure to ambient atmospheric conditions, which is mostly attributed to the ionic character of the material and its metastable structure.[39] Besides oxygen and water, UV-light can also have a negative effect on lead halide perovskites, especially for mixed halide perovskites.[40,41] Upon illumination, halide anions segregate to form regions with a different bandgap energy.[42]

Upon doping $CsPbCl_3$ with Yb, photodegradation of the PLQY becomes slower, in one example the PL intensity decayed to 20% of the original value within 90 h instead of 30 h.[19] The exact mechanism of this stabilization remains elusive to date. Potentially, Yb dopants accept the energy that would otherwise remain

View Article Online
DOI: 10.1039/D0MH01470B

in the excited states of the perovskite host causing photodegradation. In all cases, further improvement is needed for long-term applications.

Lead halide perovskites contain water-soluble Pb salts which may be able to leak into the environment. Therefore, Pb perovskites require fail-safe encapsulation before they can be commercialized.[42] Pb-free perovskites like the double-perovskites discussed above are, so far, not suitable for high-efficiency QC. The exact hazard from Pb in solar cell applications is still under fierce debate,[43] in particular given the small quantities deposited in sub-micron thick perovskite layers.

Power Saturation and Directional Emission

For applications in solar cells, the QC layer needs to work at a large range of intensities, and the emitted photons need to be directed towards the Sun. The usable intensity range is limited by the power saturation, discussed in Section 3. Considerable efforts have been undertaken towards understanding the cause and mechanism of power saturation, but real-world applications would benefit tremendously from reducing it. Guided by the results of their simulations, Erickson *et al.* devised three engineering routes to reduce saturation.[16]

The first is to reduce the Yb^{3+} lifetime. Potentially the radiative lifetime itself could be reduced by changing the local density of optical states (LDOS) close to the emitter complex as, generally, the radiative emission depends on them. Nanostructures can be used to change the LDOS, and this could potentially be a way to reduce power saturation.

The second route is to increase the concentration of Yb, which will reduce the photoexcitation rate per Yb^{3+} ion. The same result can be achieved by stacking various Yb^{3+}:$CsPb(Cl_{1-x}Br_x)_3$ layers with different bandgap energies so that the layers will filter solar flux and decrease the excitation rate in each layer.

The third route involves a change in perovskite bandgap. When starting from the $^2F_{5/2}$ excited state of Yb^{3+}, the bandgap of $CsPbX_3$ matches almost perfectly the charge-transfer transition from the halide to Yb^{3+}. Because this resonance is the largest contribution to the NC*-Yb* cross relaxation, an energy mismatch could help reduce the power saturation effect. This can be achieved by changing the bandgap of the perovskite host (for example, by changing perovskite composition). However, we think that this route may eventually decrease the population of the Yb^{3+} state in favor of the perovskite emission.

Emission of the downconverted photons is, a priori, omnidirectional. For the application with silicon solar cells, however, a large fraction needs to be directed into the solar cell. When the refractive index contrast between air and silicon is utilized to direct the emission, a large fraction (~85%) of the photons can be directed into silicon.[44] This directionality, however, requires the downconverter and silicon to be in direct contact with each other. Moreover, a loss of >10% is far from ideal. The emission of photons can also be rendered directional using asymmetric nanostructures.[45] If such nanostructures are placed asymmetrically with respect to the Yb emitters they could be used to direct the emission towards the solar cell by changing the LDOS only for certain emission k-vectors. This benefit of the nanostructures could be combined with an overall increase in the LDOS as discussed above, to overcome power saturation.

If the Yb^{3+} ions were very close to the surface of the silicon solar cell then the energy could be transferred by a Dexter-type energy transfer process.[46] This transfer would be completely non-radiative. As long as this transfer is faster than other non-radiative decays and the radiative decay, then the excitation will automatically be directed towards the solar cell. Such transfer would also reduce or even avoid power saturation because it could be designed to be much faster than the long radiative lifetime, quickly depleting the excited Yb^{3+} states.

Yb, How Rare is *Rare*?

Despite what their name suggests, RE elements are not necessarily scarce. In fact, RE elements are present in low concentrations in all minerals and are cost-effectively extracted from a selection of less common ones.[47] For example, Yb is commercially recovered from monazite sand (0.03% Yb) and found in minerals such as euxenite and xenotime. [48]

But how *rare* is Yb when related to large-scale implementation? Current Yb applications include doping of stainless steel to improve its mechanical properties, as a laser source, and in atomic clocks. However, none of these applications is implemented at mass-scale[48]

When it comes to the employment of Yb as a material for possibly widespread PV applications, a back-of-the-envelope calculation allows to assess whether its usage for PV purposes would threaten its abundance on Earth. Only taking into account the amount of Yb currently present in the upper 3 km of the Earth's crust we could cover a surface area of about $5.4 \cdot 10^{13}$ km^2 (see Supplementary Information). Putting it in perspective, this number corresponds to the surface of over 100,000 Earths.

Conclusion

We have reviewed the rise and recent development of an exciting new QC material, Yb-doped lead halide perovskites. Yb^{3+}:$CsPbX_3$ NCs (X = Cl, Br) and thin films show very high PLQYs, well exceeding 100% with a current record of 193%. These high PLQYs are due to QC, where high-energy excitations are converted into two lower-energy photons. This opens opportunities for application in downconversion, a technique where a QC layer is deposited on top of a solar cell, shaping the solar spectrum to be more suitable for the bandgap of the solar cell. The emission energy of the excited Yb^{3+} $^2F_{5/2} - {}^2F_{7/2}$ transitions is 1.26 eV, suitable for silicon solar cells which have a bandgap of 1.12 eV.

The QC in Yb^{3+}:$CsPbX_3$ occurs via a vacancy-defect complex of two Yb^{3+} ions and one vacancy, taking the place of three Pb ions in the perovskite host lattice. The vacancy introduces a defect with energy close to the conduction band of the perovskite. This defect forms an intermediate state for fast population of the $^2F_{5/2}$ excited state of the Yb^{3+} ion. The long lifetime of the $^2F_{5/2}$ state in Yb^{3+} (up to 2 ms) causes a power saturation effect which results in decreasing photoluminescence at increasing incident flux; the PLQY drops below 100% even at intensities well below one Sun. At high flux, photoluminescence from the Yb^{3+} states competes with a fast Auger-type process, which results in the loss of energy in the form of heat. However, even with saturation effects, both models and experiments show that a downconversion layer of

View Article Online
DOI: 10.1039/D0MH01470B

Yb^{3+}:$CsPbX_3$ on top of a solar cell can lead to a relative efficiency increase up to 20.6%. Especially in winter and at hours of the day with less solar irradiation, Yb^{3+}:$CsPbX_3$ can drastically improve the efficiency. Additional research should be conducted to limit the negative effects of saturation, increasing the efficiency by optimizing halide and Yb concentration, and enhancing the stability of the material. For implementation in solar cells, the directionality of the emission, or new ways to transfer the energy from the Yb^{3+} ions into the solar cell should be investigated. Overall, Yb-doped perovskites are a very promising material for solar downconversion with real potential to increase the efficiency of commercial solar cells.

Acknowledgements

This work is part of the research program of the Dutch Research Council (NWO).

References

1. Shockley, W. & Queisser, H. J. Detailed Balance Limit of Efficiency of p-n Junction Solar Cells. *J. Appl. Phys.* **32**, 510–519 (1961).
2. Richter, A., Hermle, M. & Glunz, S. W. Reassessment of the Limiting Efficiency for Crystalline Silicon Solar Cells. *IEEE J. Photovoltaics* **3**, 1184–1191 (2013).
3. Green, M. A. *et al.* Solar cell efficiency tables (version 56). *Prog. Photovoltaics Res. Appl.* **28**, 629–638 (2020).
4. Leijtens, T., Bush, K. A., Prasanna, R. & McGehee, M. D. Opportunities and challenges for tandem solar cells using metal halide perovskite semiconductors. *Nat. Energy* **3**, 828–838 (2018).
5. Pietryga, J. M. *et al.* Spectroscopic and device aspects of nanocrystal quantum dots. *Chem. Rev.* **116**, 10513–10622 (2016).
6. Beard, M. C., Luther, J. M., Semonin, O. E. & Nozik, A. J. Third generation photovoltaics based on multiple exciton generation in quantum confined semiconductors. *Acc. Chem. Res.* **46**, 1252–1260 (2013).
7. Rao, A. & Friend, R. H. Harnessing singlet exciton fission to break the Shockley-Queisser limit. *Nature Reviews Materials* **2**, 17063-1-17063–12 (2017).
8. Futscher, M. H., Rao, A. & Ehrler, B. The Potential of Singlet Fission Photon Multipliers as an Alternative to Silicon-Based Tandem Solar Cells. *ACS Energy Lett.* **3**, 2587–2592 (2018).
9. Kroupa, D. M., Roh, J. Y., Milstein, T. J., Creutz, S. E. & Gamelin, D. R. Quantum-Cutting Ytterbium-Doped CsPb(Cl1- xBrx)3 Perovskite Thin Films with Photoluminescence Quantum Yields over 190%. *ACS Energy Lett.* **3**, 2390–2395 (2018).
10. Huang, X., Han, S., Huang, W. & Liu, X. Enhancing solar cell efficiency: The search for luminescent materials as spectral converters. *Chem. Soc. Rev.* **42**, 173–201 (2013).
11. Milstein, T. J., Kroupa, D. M. & Gamelin, D. R. Picosecond Quantum Cutting Generates Photoluminescence Quantum Yields over 100% in Ytterbium-Doped CsPbCl3 Nanocrystals. *Nano Lett.* **18**, 3792–3799 (2018).
12. Crane, M. J., Kroupa, D. M. & Gamelin, D. R. Detailed-Balance Analysis of Yb3+:CsPb(Cl1-xBrx)3

Quantum-Cutting Layers for High-Efficiency Photovoltaics under Real-World Conditions. *Energy Environ. Sci.* **12**, 2486–2495 (2019).

13. Hanna, M. C. & Nozik, A. J. Solar conversion efficiency of photovoltaic and photoelectrolysis cells with carrier multiplication absorbers. *J. Appl. Phys.* **100**, 074510-1-074510–8 (2006).
14. Pan, G. *et al.* Doping Lanthanide into Perovskite Nanocrystals: Highly Improved and Expanded Optical Properties. *Nano Lett.* **17**, 8005–8011 (2017).
15. Li, X. *et al.* Mechanism for the Extremely Efficient Sensitization of Yb 3+ Luminescence in CsPbCl 3 Nanocrystals. *J. Phys. Chem. Lett.* **10**, 487–492 (2019).
16. Erickson, C. S., Crane, M. J., Milstein, T. J. & Gamelin, D. R. Photoluminescence Saturation in Quantum-Cutting Yb3+-Doped CsPb(Cl1- xBrx)3 Perovskite Nanocrystals: Implications for Solar Downconversion. *J. Phys. Chem. C* **123**, 12474–12484 (2019).
17. Cohen, T. A. *et al.* Quantum-cutting Yb3+-doped perovskite nanocrystals for monolithic bilayer luminescent solar concentrators. *J. Mater. Chem. A* **7**, 9279–9288 (2019).
18. Zhou, D. *et al.* Cerium and Ytterbium Codoped Halide Perovskite Quantum Dots: A Novel and Efficient Downconverter for Improving the Performance of Silicon Solar Cells. *Adv. Mater.* **29**, 1–6 (2017).
19. Zhang, X. *et al.* Yb3+ and Yb3+/Er3+ doping for near-infrared emission and improved stability of CsPbCl3 nanocrystals. *J. Mater. Chem. C* **6**, 10101–10105 (2018).
20. Zhou, D. *et al.* Impact of Host Composition, Codoping, or Tridoping on Quantum-Cutting Emission of Ytterbium in Halide Perovskite Quantum Dots and Solar Cell Applications. *Nano Lett.* **19**, 6904–6913 (2019).
21. Ma, J. P. *et al.* Insights into the local structure of dopants, doping efficiency, and luminescence properties of lanthanide-doped CsPbCl3 perovskite nanocrystals. *J. Mater. Chem. C* **7**, 3037–3048 (2019).
22. Luo, X., Ding, T., Liu, X., Liu, Y. & Wu, K. Quantum-Cutting Luminescent Solar Concentrators Using Ytterbium-Doped Perovskite Nanocrystals. *Nano Lett.* **19**, 338–341 (2019).
23. Mir, W. J. *et al.* Postsynthesis Doping of Mn and Yb into CsPbX3 (X = Cl, Br, or I) Perovskite Nanocrystals for Downconversion Emission. *Chem. Mater.* **30**, 8170–8178 (2018).
24. Crane, M. J. *et al.* Single-Source Vapor Deposition of Quantum-Cutting Yb 3+ :CsPb(Cl 1– x Br x) 3 and Other Complex Metal-Halide Perovskites. *ACS Appl. Energy Mater.* **2**, 4560–4565 (2019).
25. Mahor, Y., Mir, W. J. & Nag, A. Synthesis and Near Infrared Emission of Yb Doped Cs 2 AgInCl 6 Double Perovskite Microcrystals and Nanocrystals. *J. Phys. Chem. C* **123**, 15787–15793 (2019).
26. Lee, W., Hong, S. & Kim, S. Colloidal Synthesis of Lead-Free Silver-Indium Double-Perovskite Cs 2 AgInCl 6 Nanocrystals and Their Doping with Lanthanide Ions. *J. Phys. Chem. C* **123**, 2665–2672 (2019).
27. Hu, Q. *et al.* Rare Earth Ion-Doped CsPbBr3 Nanocrystals. *Adv. Opt. Mater.* **6**, 1–5 (2018).
28. Chen, N. *et al.* Yb- and Mn-Doped Lead-Free Double Perovskite Cs 2 AgBiX 6 (X = Cl - , Br -) Nanocrystals. *ACS Appl. Mater. Interfaces* **11**, 16855–16863 (2019).
29. Milstein, T. J. *et al.* Anion Exchange and the Quantum-Cutting Energy Threshold in Ytterbium-Doped CsPb(Cl 1- x Br x) 3 Perovskite Nanocrystals. *Nano Lett.* **19**, 1931–1937 (2019).

30. Kangsabanik, J., Sugathan, V., Yadav, A., Yella, A. & Alam, A. Double perovskites overtaking the single perovskites: A set of new solar harvesting materials with much higher stability and efficiency. *Phys. Rev. Mater.* **2**, 1–12 (2018).
31. Khalfin, S. & Bekenstein, Y. Advances in lead-free double perovskite nanocrystals, engineering band-gaps and enhancing stability through composition tunability. *Nanoscale* **11**, 8665–8679 (2019).
32. Sadhanala, A. *et al.* Blue-Green Color Tunable Solution Processable Organolead Chloride-Bromide Mixed Halide Perovskites for Optoelectronic Applications. *Nano Lett.* **15**, 6095–6101 (2015).
33. Green, M. A. *et al.* Solar cell efficiency tables (version 56). *Prog. Photovoltaics Res. Appl.* **28**, 629–638 (2020).
34. Ferreira, R. A. S., Correia, S. F. H., Monguzzi, A., Liu, X. & Meinardi, F. Spectral converters for photovoltaics – What's ahead. *Mater. Today* **33**, 105–121 (2020).
35. Mir, W. J., Sheikh, T., Arfin, H., Xia, Z. & Nag, A. Lanthanide doping in metal halide perovskite nanocrystals: spectral shifting, quantum cutting and optoelectronic applications. *NPG Asia Mater.* **12**, 9-1-9–9 (2020).
36. Pan, G. *et al.* Impurity Ions Codoped Cesium Lead Halide Perovskite Nanocrystals with Bright White Light Emission toward Ultraviolet–White Light-Emitting Diode. *ACS Appl. Mater. Interfaces* **10**, 39040–39048 (2018).
37. Ishii, A. & Miyasaka, T. Sensitized Yb3+ Luminescence in CsPbCl3 Film for Highly Efficient Near-Infrared Light-Emitting Diodes. *Adv. Sci.* **7**, 1–7 (2020).
38. Nie, W. *et al.* Light-activated photocurrent degradation and self-healing in perovskite solar cells. *Nat. Commun.* **7**, 11574-1-11574–9 (2016).
39. Woo, J. Y. *et al.* Highly Stable Cesium Lead Halide Perovskite Nanocrystals through in Situ Lead Halide Inorganic Passivation. *Chem. Mater.* **29**, 7088–7092 (2017).
40. Niu, G. *et al.* Study on the stability of CH3NH3PbI3 films and the effect of post-modification by aluminum oxide in all-solid-state hybrid solar cells. *J. Mater. Chem. A* **2**, 705–710 (2014).
41. Leijtens, T. *et al.* Overcoming ultraviolet light instability of sensitized TiO2 with meso-superstructured organometal tri-halide perovskite solar cells. *Nat. Commun.* **4**, 1–8 (2013).
42. Slavney, A. H. *et al.* Chemical Approaches to Addressing the Instability and Toxicity of Lead-Halide Perovskite Absorbers. *Inorg. Chem.* **56**, 46–55 (2017).
43. Ke, W. & Kanatzidis, M. G. Prospects for low-toxicity lead-free perovskite solar cells. *Nat. Commun.* **10**, 1–4 (2019).
44. Nguyen, H. M. *et al.* Efficient radiative and nonradiative energy transfer from proximal CdSe/ZnS nanocrystals into silicon nanomembranes. *ACS Nano* **6**, 5574–5582 (2012).
45. Bidault, S., Mivelle, M. & Bonod, N. Dielectric nanoantennas to manipulate solid-state light emission. *J. Appl. Phys.* **126**, 094104-1-094104–16 (2019).
46. Dexter, D. L. A Theory of Sensitized Luminescence in Solids. *J. Chem. Phys.* **21**, 836 (1953).
47. Balaram, V. Rare earth elements: A review of applications, occurrence, exploration, analysis, recycling, and environmental impact. *Geosci. Front.* **10**, 1285–1303 (2019).
48. Encyclopedia Britannica, Ytterbium, https://www.britannica.com/science/ytterbium, (accessed September 07, 2020)

View Article Online
DOI: 10.1039/D0MH01470B